Mon. Not. R. astr. Soc. (1982) **199**, 735–761

On solar models and their periods of oscillation

Jørgen Christensen-Dalsgaard *Department of Applied Mathematics and Theoretical Physics, University of Cambridge, England; Astronomisk Institut, Aarhus Universitet, Denmark; Institut d'Astrophysique, Liège, Belgium; and National Center for Atmospheric Research, PO Box 3000, Boulder, CO 80307*★†

Received 1981 October 13; in original form 1978 December 7

Summary. Accurate calculations of solar models and their oscillation periods are needed if the observed oscillation periods of the Sun are to be used to infer properties of the solar interior. The paper describes a new programme for calculation of solar evolution sequences; an analysis of the numerical accuracy of the computed models is given, and the effects of changing the opacity interpolation or opacity tables are investigated. In addition selected periods of adiabatic oscillations for the models are calculated and the errors in these periods estimated. For the modes corresponding to the observed whole disc 5 min oscillations the relative error in the computed periods, given the physics in the model calculation, is around 1.7×10^{-3}. This value is significantly smaller than the difference in periods between models computed with the Cox & Tabor (1976) and the Carson (1976) opacities.

1 Introduction

There is mounting observational evidence for the existence of large-scale solar oscillations (e.g. Brown, Stebbins & Hill 1978; Kotov, Severny & Tsap 1978; Claverie *et al.* 1979, 1980; Scherrer *et al.* 1979, 1980; Caudell *et al.* 1980; Grec, Fossat & Pomerantz 1980). Such observations may enable helio-seismological investigations, where a comparison between observed periods of oscillation and periods calculated from solar models are used to get information about the interior of the Sun (Scuflaire *et al.* 1975; Christensen-Dalsgaard & Gough 1976). There is evident need for such information. Apart from the periods of oscillation the only genuine test of theoretical solar models is provided by the observed capture rate of neutrinos originating from the nuclear reactions near the centre of the Sun (e.g. Bahcall & Davis 1976). Despite persistent efforts (e.g. Bahcall *et al.* 1973; Bahcall 1977) the computed capture rate has remained significantly higher than the observed value; and although the recent possible detection of neutrino oscillations (Reines, Sobel & Pasierb

★ Present address.

† The National Center for Atmospheric Research is sponsored by the National Science Foundation.

1980; Barger, Whisnant & Phillips 1980) would reduce the computed capture rate, this is partly compensated for by modifications in opacity tables and nuclear reaction rates (Bahcall *et al.* 1980), so that the problem may remain. An independent test of the models is therefore badly needed. Such a test clearly affects the whole theory of low-mass stellar evolution and thus has ramifications for a wide area of astrophysics.

Some inferences about solar structure, based on observations of solar oscillations, have already been made. The detailed observations of 5 min oscillations of high degree (Deubner 1975; Rhodes, Ulrich & Simon 1977; Deubner, Ulrich & Rhodes 1979) agree reasonably well with calculated frequencies of solar envelope models, provided these have a sufficiently deep convection zone (Berthomieu *et al.* 1980; Lubow, Rhodes & Ulrich 1980); these modes, however, give no direct information about the layers beneath the convection zone. A somewhat deeper probe is provided by the 5 min oscillations of low degree observed by Claverie *et al.* and Grec *et al.*; these include radial modes which penetrate to the centre of the model, although their periods are largely determined by the structure of the convection zone. The mean frequency separation observed for these modes is in good agreement with the values calculated for traditional solar models (Christensen-Dalsgaard & Gough 1980b). Due to their very high frequency resolution the observations by Grec *et al.* give detailed information about these modes; in particular it is possible to determine their degree l and thus to make an identification between the observed modes and modes computed for solar models. It remains to be seen whether the accuracy of the observed periods is sufficient to get detailed information about the deep solar interior; as discussed in Section 6.5 it may at least be possible to put constraints on the degree of mixing in the core of the Sun.

Modes with longer periods are generally more sensitive to conditions in the solar interior. Such modes have apparently been observed (Brown *et al.* 1978; Caudell *et al.* 1980; Scherrer *et al.* 1979, 1980), but so far no compelling observational determination of their horizontal structure has been made, and so their usefulness for helio-seismology is as yet limited. On the other hand modes of longer period generally preserve phase over much longer time intervals than the 5 min modes discussed above, and so their periods can be determined with greater accuracy. The results of Scherrer *et al.* (1980) indicate that one such mode, with a period close to 160 min, has preserved its phase over six years, so that its period should now be determined to within a relative error of about 5×10^{-5}; identification of this mode with a specific mode of oscillation in a solar model would thus give information of very high accuracy related to the interior structure of the Sun.

To fully utilize such observations the accuracy of the computed periods, given the physical assumptions entering the calculation of the model, should be comparable with the observational accuracy. Indeed such accuracy is probably needed if the 5 min oscillations of low degree are to be used to distinguish between different traditional solar models (*cf.* Christensen-Dalsgaard & Gough 1980b). It is not clear that present solar models meet this standard of accuracy. Although the neutrino problem has led to careful computation of a large number of solar models (see e.g. Bahcall *et al.* 1969, 1973; Abraham & Iben 1971), these calculations have placed the greatest emphasis on the structure of the energy generating region of the model, which on the whole determines the neutrino flux for models having the correct surface luminosity. On the other hand periods of oscillation of a solar model are sensitive to the structure of the model as a whole. Thus when constructing a model in order to analyse its modes of oscillation, care must be taken to ensure that all parts of the model are adequately dealt with; in particular the mesh used for the numerical solution of the equations of stellar evolution must have a reasonable distribution of points.

The present paper describes a solar evolution programme which attempts to meet the standard of accuracy promised by the observations of solar oscillations. The programme

drew some inspiration from the calculations by Eggleton (1971, 1972), but is otherwise completely independent of existing programmes. Thus it seems reasonable to describe the calculation in some detail, even where it does not depart significantly from previous work. Section 2 presents the physical basis for the calculation, and Section 3 discusses the numerical techniques, whereas Appendix A, B and C describe the central boundary conditions, the difference equations used to discretize the equations of stellar evolution, and the scheme used to set the distribution of mesh points. Results of the evolution calculations are presented in Section 4.

Most of the observed oscillation periods correspond to modes of fairly high radial order, and so the period calculation requires some care. In addition it is clearly of great interest to determine the effect on the periods of errors in the model calculation. Section 5 addresses these questions, with Appendix D giving further details about the computational methods and their inherent errors. Finally, Section 6 discusses the results, with particular emphasis on the prospects for helio-seismology, and Section 7 contains a brief conclusion.

2 Equations and boundary conditions

We assume that the effect on the solar models of rotation and large-scale magnetic fields can be neglected; thus in particular the models are spherically symmetric. This assumption is supported, for the present Sun at least, by the observations of Hill & Stebbins (1975), showing an oblateness of the solar surface consistent with what is caused by the effect on the solar surface of the centrifugal force due to the observed surface rotation rate.

We neglect the effect of mass loss and accretion. None of the models have a convective core or an outer convection zone extending to the region where the chemical composition has been modified by nuclear burning. As we ignore all other sources of mixing the composition is only affected locally by the nuclear reactions; in particular the surface composition is unchanged during the evolution.

The CN cycle is assumed to be always in nuclear equilibrium. On the other hand the departure of ^{3}He from nuclear equilibrium has a significant effect on the stability towards non-radial oscillations of the models during the first few hundred million years (*cf.* Christensen-Dalsgaard, Dilke & Gough 1974), and for this reason we have computed the evolution with time of X_3, the ^{3}He abundance by mass.

The effect on the thermodynamic state and on the opacity of the variation throughout the model in the abundances of all other elements than ^{1}H and ^{4}He is neglected. Hence for the purpose of calculating the thermodynamic functions and the opacity the composition is specified by X and Y, the abundances by mass of ^{1}H and ^{4}He respectively, with $X + Y = 1 - Z$ being the same throughout the model; here Z is the total abundance by mass of all other elements. Thus the composition is described by the variables X and X_3, as well as Z which is a parameter of the calculation.

We choose as independent variable $x = \log q$, where log is the logarithm to base 10 and $q = m/M$, m being the mass in the model interior to the point considered and M the total mass of the model. The equations of stellar evolution (e.g. Clayton 1968), given the assumptions made above, are then formulated in terms of the dependent variables $y_1 = \log r$, $y_2 = \log p$, $y_3 = \log T$, $y_4 = \log L$, $y_5 = X$ and $y_6 = X_3$; here r is the distance to the centre of the model, p and T are pressure and temperature, and L is the flow of energy per unit time through a sphere of radius r. These quantities clearly satisfy a set of partial differential equations in x and time t.

To complete the equations we need auxiliary expressions for the thermodynamic state, energy generation and opacity. The thermodynamic functions are calculated using the

formulation described by Eggleton, Faulkner & Flannery (1973), giving fairly accurate and thermodynamically consistent expressions for density, electron pressure and electron enthalpy for a partially ionized, partially degenerate gas, as explicit functions of T, composition and a quantity f related to the electron degeneracy parameter. We include the crude approximation to 'pressure ionization' proposed by Eggleton *et al.*; this has the merit of being thermodynamically consistent and ensuring complete ionization in the interior of the model, while still allowing explicit calculation of the thermodynamic state in terms of f, T and composition.

All atoms and ions were assumed to be in their ground states. Thus the partition functions were approximated by the statistical weights of the ground states, and the contribution to the internal energy of the gas from the excitation energy was neglected. To find the number of electrons and the ionization energy contributed by the heavy elements the state of ionization of C and O was calculated in detail, and the metals were approximated by Fe, including only the outermost electron. This approximation has been compared with a detailed ionization calculation involving the 10 most abundant elements, with the relative composition given by Ross & Aller (1976). To calibrate the approximation the abundances of C, O and Fe were adjusted to obtain the best possible agreement in electron number throughout a typical solar model; the error in the number of electrons contributed by the heavy elements was at most 3 per cent, and less than 1 per cent above the hydrogen ionization zone, where the heavy elements provide all the free electrons. In view of the small total abundance of heavy elements this is entirely adequate.

We use the diffusion approximation to describe the flow of energy in regions stable towards convection; in convective regions (defined using Schwarzschild's criterion) the temperature gradient is calculated from the local mixing-length theory of Böhm-Vitense (1958) in the form used by Baker & Temesváry (1966), with a mixing length of α pressure scale heights.

Spectroscopic observations show that in the surface layers of the present Sun $Z/X \simeq 0.023$ (Ross & Aller 1976); as X is typically 0.73 this implies that Z is about 0.017. To avoid interpolation in Z we have nevertheless used $Z = 0.02$ for which tables of the opacity κ were available. Two different sets of tables have been used. One (referred to in the following as CT76) consisted of the tables for compositions King IIIA, King IVA and King VA (with $X = 0.6$, 0.7 and 0.8, respectively) from Cox & Tabor (1976), combined with the tables for $X = 0.5$, 0.2 and 0 from Cox & Stewart (1970); this combination was necessitated by the fact that Cox & Tabor have no tables with $Z = 0.02$ and $X \leqslant 0.5$. The second set (in the following Crs76) is based on unpublished calculations by Carson (*cf.* Carson 1976).

Interpolation of $\log\kappa$ in $\log\rho$ (ρ being the density) and $\log T$ was performed using splines under tension (Cline 1974). This method is characterized by a tension parameter η, such that $\eta = 0$ corresponds to ordinary cubic spline interpolation, whereas for very large η one gets approximately linear interpolation. By choosing a suitable intermediate value of η one can obtain a smoothly varying interpolating function without introducing the exaggerated fluctuations sometimes caused by high order polynomial interpolation. In most of the calculations reported here $\eta = 5$ was used. Due to the small number of values of X for which opacity tables were available simple quadratic interpolation in X was used.

Nuclear reaction rates were taken from Fowler, Caughlan & Zimmerman (1975) and corrected for electron screening in the weak screening approximation (Salpeter 1954). The rate of electron capture by ^{7}Be was found using the expressions in Iben, Kalata & Schwartz (1967). We used Bahcall's (1977) cross-sections to calculate the neutrino capture rates expected for the models.

It should be noticed that all physical quantities needed in the calculation can be

computed explicitly from a new set of dependent variables $\{z_i\}$ defined by

$$z_i = y_i, \quad i = 1, 3, 4, 5, 6; \qquad z_2 = \log f; \tag{2.1}$$

these are related to the y_i by a non-singular transformation $y_i = y_i(z_j)$ which can also be computed explicitly.

The equations must be supplemented by four boundary conditions. The surface of the model, where $x = 0$, is taken as corresponding to $T = T_{\rm eff}$, the effective temperature; at this point one condition is thus clearly

$$4\pi r^2 \sigma T^4 = L \qquad \text{at } x = 0 \tag{2.2}$$

where σ is the Stefan–Boltzman constant. A second condition is obtained by equating the pressure at $x = 0$ to the pressure obtained by integrating the equation of hydrostatic support in the atmosphere, assuming gravity to be constant. The dependence of $T/T_{\rm eff}$ on optical depth τ, defined using the Rosseland mean opacity, is taken from an analytical fit (Gough, private communication) to the HSRA (Gingerich *et al.* 1971) out to $\tau = 10^{-4}$; further out T is assumed to be constant.

Boundary conditions at the innermost point, $x = x_1$ say, are obtained from expansions at the centre. By expanding p, T, X and X_3 in powers of r, around $r = 0$, we get a set of non-linear algebraic equations relating the central values p_c, T_c, X_c and X_{3c} of these variables to their values at $x = x_1$. The expansions of m and L can be expressed in terms of p_c, T_c, X_c and X_{3c}, and by equating these expansions to the values of m and L at $x = x_1$ two conditions are obtained at this point. The expansion coefficients are presented in Appendix A. As a result of this procedure we get consistent values of the second derivatives of p, T, X and X_3 at the centre; these are needed in the central boundary conditions for pulsation calculations (e.g. Christensen-Dalsgaard *et al.* 1974).

Ideally the calculation should be started during the contraction phase before nuclear reactions set in, where the composition can still be assumed to be uniform. However, this appears unnecessary for an investigation whose main aim is to produce models of the present Sun. Instead we assume the initial model to be static and in thermal equilibrium, with a homogeneous hydrogen abundance $X = X_0$. To mimic the production of ^{3}He during the contraction phase the ^{3}He abundance in the initial model is taken to be the abundance resulting from ^{3}He production during a time $t_{^3\rm He}$ at constant temperature and density, assuming zero initial abundance (see e.g. Christensen-Dalsgaard *et al.* 1974). For $t_{^3\rm He} = (2\text{–}5) \times 10^7$ yr this gave an abundance which was at least qualitatively in agreement with the ^{3}He abundance found by Iben (1965) in his $1\,M_\odot$ model on its arrival on the main sequence. Furthermore the structure of models older than 5×10^8 yr was hardly affected by varying $t_{^3\rm He}$ from 2.5×10^6 to 5×10^7 yr. In the present calculations we used $t_{^3\rm He} = 5 \times 10^7$ yr.

The models were calibrated in X_0 and α to obtain a surface radius $r_\odot = 6.9599 \times 10^{10}$ cm and surface luminosity $L_\odot = 3.826 \times 10^{33}$ erg s^{-1} (Allen 1973) at the age $t_\odot = 4.75 \times 10^9$ yr. This calibration requires knowledge of the derivatives of α and X_0 with respect to the radius $r_{\rm s,\,pres}$ and luminosity $L_{\rm s,\,pres}$ of the model of the present Sun. We have used the values

$$\left.\begin{aligned} \left(\frac{\partial \ln \alpha}{\partial \ln L_{\rm s,\,pres}}\right)_{r_{\rm s,\,pres}} &= 1.24, & \left(\frac{\partial \ln \alpha}{\partial \ln r_{\rm s,\,pres}}\right)_{L_{\rm s,\,pres}} &= -4.91 \\ \left(\frac{\partial \ln X_0}{\partial \ln L_{\rm s,\,pres}}\right)_{r_{\rm s,\,pres}} &= -0.148, & \left(\frac{\partial \ln X_0}{\partial \ln r_{\rm s,\,pres}}\right)_{L_{\rm s,\,pres}} &= -0.010, \end{aligned}\right\} \tag{2.3}$$

which were derived from three evolution sequences computed with Eggleton's (1971) programme; these values gave convergence to within 5×10^{-5} in $r_{\rm s,\,pres}$ and $L_{\rm s,\,pres}$ in only three or four iterations.

3 Numerical techniques

The numerical problem can be formulated as follows: compute the solution $z_i(x, t^{s+1})$ to the equations and boundary conditions at a time level t^{s+1}, given the solution at the earlier time level t^s. This is solved using the technique of finite differences, applied to studies of stellar evolution by Henyey *et al.* (1959). Derivatives with respect to x are replaced by centred differences on a discrete mesh $\{x^n\}$, $n = 1, \ldots, N$, and time derivatives by centred or backward differences between the time levels t^s and t^{s+1}. When combined with the boundary conditions the result is a set of non-linear algebraic equations for $z_i(x^n, t^{s+1})$, which is solved by Newton–Raphson iteration. The difference equations are presented, and the method of their solution briefly discussed, in Appendix B.

It was found that stability required the use of backward differences to represent the time derivatives in the energy equation and the equation for the change in X_3. In the latter case this is due to the fact that the time step is generally much longer than the nuclear time-scale for ^{3}He in regions where ^{3}He is in nuclear equilibrium; at the centre of the model representing the present Sun this time-scale is about 10^5 yr. In the energy equation the problem is the general smallness of the rate of release of gravitational energy compared with the nuclear energy generation rate; this causes a near lack of coupling between the luminosity and the change in pressure and temperature with time, permitting an oscillation in these quantities between consecutive time levels. Calculations where thermal equilibrium was artificially destroyed indicated that this problem does not occur when the rates of gravitational and nuclear energy generation are comparable. Main sequence evolution is of course very largely controlled by the change in the hydrogen abundance, and so it is not surprising that use of centred differences caused no problems in the equation for X.

The programme used to set up and solve the difference equations and boundary conditions is written in a sufficiently flexible way to allow it to solve any set of partial differential equations of the same general form as the equations of stellar evolution (see equations (B1)–(B3) in Appendix B). Thus it was possible to test it on problems with known solutions, like the one-dimensional diffusion equation and the wave equation.

The distribution of the mesh points in x is determined using a method very similar to the first derivative stretching introduced by Gough, Spiegel & Toomre (1975). In particular the variation of the superadiabatic temperature gradient $\nabla - \nabla_{ad}$ is taken into account, thus ensuring a reasonable resolution of the region of large superadiabaticity near the top of the convection zone. Typically about half the mesh points are in the convection zone and about 10 per cent in the region betweeen the surface and the maximum in $\nabla - \nabla_{ad}$. The position of the innermost mesh point is determined from the ratios between central values and second derivatives at the centre of p, T, X, m/r^3 and L/r^3. The parameters are chosen such that the separation $r_2 - r_1$ in r between the innermost two mesh points is about $0.09\, r_1$. Finally the time step $\Delta t^{s+1} = t^{s+2} - t^{s+1}$ is found from the maximum change in the solution from time level t^s to time level t^{s+1}.

The expressions used to determine the mesh and the time step are set out in Appendix C.

4 Results of the model calculations

Four calibrated evolution sequences of solar models (models 1–4) were computed. The time step for these was determined with $\Delta y_{max} = 0.1$ in equation (C4), resulting in a total of 14 time steps from the initial model to the model of the present Sun. To estimate the effect of truncation in time an additional uncalibrated sequence (model 1a), with $\Delta y_{max} = 0.05$, was calculated using the same α and X_0 as model 1. Some characteristics of the sequences are presented in Table 1.

Table 1. Properties of the evolution sequences, N is the number of mesh points, and Δy_{max} determines the time step (*cf.* equation C4); η is the tension in the opacity interpolation, X_0 the initial hydrogen abundance, α the ratio of mixing length to pressure scale height, and $r_{s,ZAMS}$ and $L_{s,ZAMS}$ are the surface radius and luminosity of the initial model. The remaining quantities refer to the model of age 4.75×10^9 yr; r_s and L_s are surface radius and luminosity, X_c, T_e and ρ_c are central hydrogen abundance, temperature and density, D is the depth of, and $1-q_B$ the mass fraction contained in, the convection zone, and T_B is the temperature at the base of the convection zone.

	Model 1	Model 1a	Model 2	Model 3	Model 4
N	201	201	401	201	201
Δy_{max}	0.1	0.05	0.1	0.1	0.1
Opacity table	CT76	CT76	CT76	CT76	Crs76
η	5	5	5	40	5
X_0	0.7335	0.7335	0.7330	0.7270	0.7306
α	1.6364	1.6364	1.6334	1.5931	1.9279
$r_{s,ZAMS}$ (cm)	6.1350×10^{10}	6.1350×10^{10}	6.1365×10^{10}	6.1415×10^{10}	6.1852×10^{10}
$L_{s,ZAMS}$ (erg s^{-1})	2.7250×10^{33}	2.7250×10^{33}	2.7239×10^{33}	2.7399×10^{33}	2.7062×10^{33}
Present Sun					
r_s (cm)	6.9599×10^{10}	6.9588×10^{10}	6.9598×10^{10}	6.9598×10^{10}	6.9599×10^{10}
L_s (erg s^{-1})	3.8262×10^{33}	3.8248×10^{33}	3.8259×10^{33}	3.8262×10^{33}	3.8261×10^{33}
X_c	0.3776	0.3778	0.3775	0.3678	0.3680
T_c (K)	14.835×10^6	14.834×10^6	14.834×10^6	14.966×10^6	15.137×10^6
ρ_c (g cm^{-3})	150.62	150.53	150.64	149.49	147.32
D/r_s	0.2828	0.2828	0.2826	0.2741	0.2517
$1-q_B$	0.0219	0.0219	0.0217	0.0194	0.0149
T_B	2.145×10^6	2.145×10^6	2.141×10^6	2.065×10^6	1.834×10^6
Neutrino capture rates					
^{8}B	4.14	4.12	4.14	4.88	5.39
^{7}Be	0.85	0.85	0.85	0.91	0.91
pep	0.22	0.22	0.22	0.22	0.22
CNO	0.18	0.18	0.18	0.21	0.22
Total	5.39	5.38	5.40	6.22	6.74

4.1 NUMERICAL ACCURACY

To investigate the effects of the truncation error* in x on the properties of the ZAMS models we computed four models with the same parameters as model 2 of Table 1, on meshes having the same distribution, but varying number N, of points (the distribution of points being slightly different from that used for model 2). The results are shown in Table 2. As the difference scheme is of second order in x, the values of r_s and L_s for an infinitely fine mesh can be estimated from the corresponding values at $N = 201$ and 401 by Richardson extrapolation as, for example

$$r_s(\infty) \simeq \tfrac{1}{3}\,[4r_s(401) - r_s(201)], \tag{4.1}$$

where $r_s(N)$ is the value of r_s found with a mesh having N points. The values of $r_s(\infty)$ and $L_s(\infty)$ are shown in the row marked R. Estimates $E(r_s; N)$ and $E(L_s; N)$ of the relative errors in r_s and L_s, normalized to a mesh with 201 points, can be defined by, for example,

$$E(r_s; N) = [r_s(N)/r_s(\infty) - 1]\,[(N-1)/200]^2; \tag{4.2}$$

these are also shown in the table. For a second-order scheme $E(r_s; N)$ and $E(L_s; N)$ are expected to be independent of N; this is roughly confirmed by Table 2, which also shows

* Here and in the following the term 'truncation error' refers, as usual, to the error in the solution caused by the replacements of derivatives by finite differences.

Table 2. Surface radius (r_s) and luminosity (L_s) of chemically homogeneous, static models computed with different numbers N of mesh points. $E(r_s; N)$ and $E(L_s; N)$ are estimates of the relative errors in r_s and L_s, and $E_{max}(p; N)$ is an estimate of the maximum relative error in p, all for a model with $N = 201$.

N	r_s (cm)	L_s (erg s^{-1})	$E(r_s; N)$	$E(L_s; N)$	$E_{max}(p; N)$
151	6.1420×10^{10}	2.7407×10^{33}	6.3×10^{-4}	4.0×10^{-3}	1.9×10^{-2}
201	6.1379×10^{10}	2.7322×10^{33}	4.6×10^{-4}	4.1×10^{-3}	2.2×10^{-2}
301	6.1365×10^{10}	2.7261×10^{33}	3.9×10^{-4}	3.2×10^{-3}	1.8×10^{-2}
401	6.1358×10^{10}	2.7239×10^{33}	4.6×10^{-4}	4.1×10^{-3}	—
R	6.1351×10^{10}	2.7212×10^{33}	—	—	—

that the relative errors in r_s and L_s for a mesh with 201 points is about 5×10^{-4} and 4×10^{-3}, respectively.

An indication of the errors in the interior of the models is given by the maximum relative difference $\Delta_{max}(p; N)$ in p between the model with N, and the model with 401, points; the corresponding estimate

$$E_{max}(p; N) = \Delta_{max}(p; N) \Big/ \left[\left(\frac{200}{N-1}\right)^2 - \frac{1}{4}\right] \tag{4.3}$$

of the maximum relative error in p in a model with 201 points is shown in Table 2. The maximum relative errors in ρ and T are considerably smaller, about 10^{-2} and 7×10^{-3} respectively.

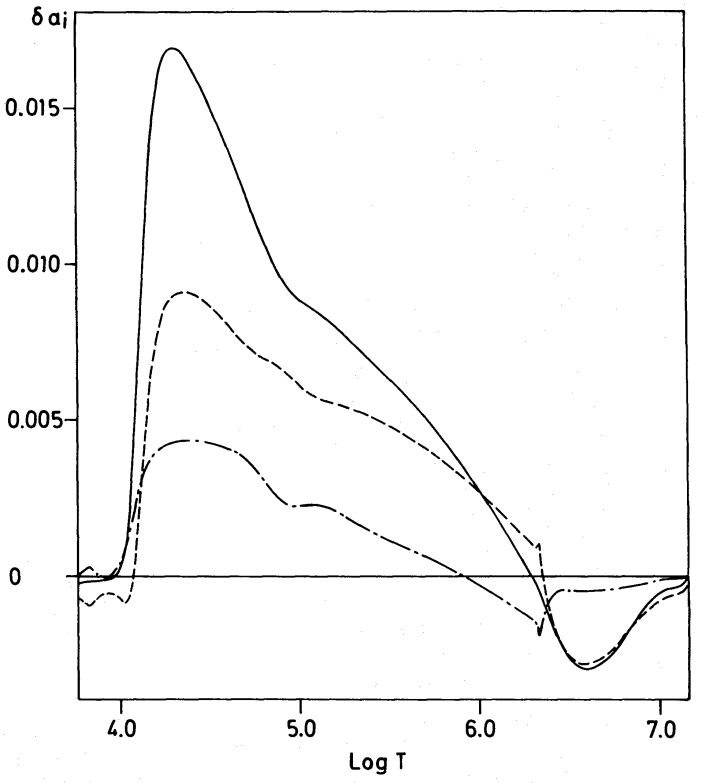

Figure 1. Differences between models 1 and 2, at fixed mass fraction q, in $a_1 = \ln p$ (——), $a_2 = \ln \rho$ (– – –) and $a_3 = \ln T$ (– · – · –), ln being the natural logarithm. The abscissa is the logarithm, to base 10, of the temperature.

A comparison between models 1 and 2 shows that the truncation error in x has minor effect on the 'global' properties of a calibrated model of the present Sun. The behaviour in the interior of the model of the relative differences between models 1 and 2 in p, ρ and T are shown on Fig. 1. The maximum relative difference in p, about 1.7×10^{-2}, corresponds to a maximum relative error in p of about 2.3×10^{-2} in model 1, similar to the values in Table 2. The relative errors in p, ρ and T are less than 10^{-2} in the inner 95 per cent by radius of the model. This distribution of error of course reflects the choice of parameters w_i in equation (C2) defining the mesh; thus by increasing w_2 or w_3, and hence the effect of p or T on the mesh, one might presumably reduce the maximum error in p. On the other hand the fact that the errors are large only rather close to the surface reduces their effect on the computed eigenfrequencies of the model; this is confirmed by the results of Section 5.

A comparison of models 1 and 1a shows that a doubling of the number of time steps results in a relative change in the surface radius and luminosity of 1.6×10^{-4} and 3.8×10^{-4}, respectively. The maximum relative change in pressure and density is 8×10^{-4}, the change in temperature being even smaller. Thus in the present calculation the effects of truncation in time are far smaller than the effects of spatial truncation.

It is of some interest to investigate the behaviour of the solution very close to the centre. The coefficients in the expansion of p around $r = 0$, truncated after the term in r^4, can be expressed in terms of the central values ρ_c and ρ_2 of the density and its second derivative (*cf.* equation A4). Using this expansion one may estimate ρ_c and ρ_2 from the values of p at the three points closest to, but excluding, the centre. When applied to model 1 of the present Sun this procedure yields values of ρ_c and ρ_2 within 0.1 and 10 per cent, respectively, of the values obtained directly from the expansion of ρ around the centre. A similar calculation for a model computed with Eggleton's (1971) programme yielded a value of ρ_c which was 13 per cent smaller than the value obtained by extrapolating ρ to the centre, whereas ρ_2 was found to have the wrong sign. This indicates an inconsistency in the behaviour of p close to the centre of the model; it is probably entirely harmless for general calculations of stellar evolution, but it may have some effect on calculations of the oscillations of the model. Thus the careful treatment, in the present calculation, of the central boundary condition appears to be warranted.

4.2 THE TREATMENT OF THE OPACITY

Some effects of using linear rather than spline interpolation in the opacity tables can be seen by comparing models 1 and 3. As was also found by Abraham & Iben (1971) linear interpolation increases the central temperature, and hence the neutrino flux, of the model. In the regions corresponding to the central parts of the model $\log \kappa$ is concave as a function both of $\log \rho$ and $\log T$ and is therefore overestimated by linear interpolation; this causes an increase in temperature. Relative differences in p, ρ and T between models 3 and 1 are shown in Fig. 2. The effect of linear opacity interpolation is largest in the deep interior of the model where the mesh used in the opacity tabulation is relatively widely spaced; here differences of up to about 3 per cent in p, ρ and T are found. In the adiabatic part of the convection zone the structure is not directly affected by the opacity, and close to the surface the differences are small, due to the dense mesh in the corresponding region of the opacity tables.

Finally a comparison of models 1 and 4 shows how the model is affected if the Cox & Tabor (1976) opacity tables are replaced by those of Carson (1976); Fig. 3 presents differences in $\ln p$, $\ln \rho$ and $\ln T$ between these two models. The dominant feature is that the surface pressure and density in model 4 is lower by a factor of about 1.5 than the corresponding quantities in model 1. This is caused by the fact that the Carson opacities at

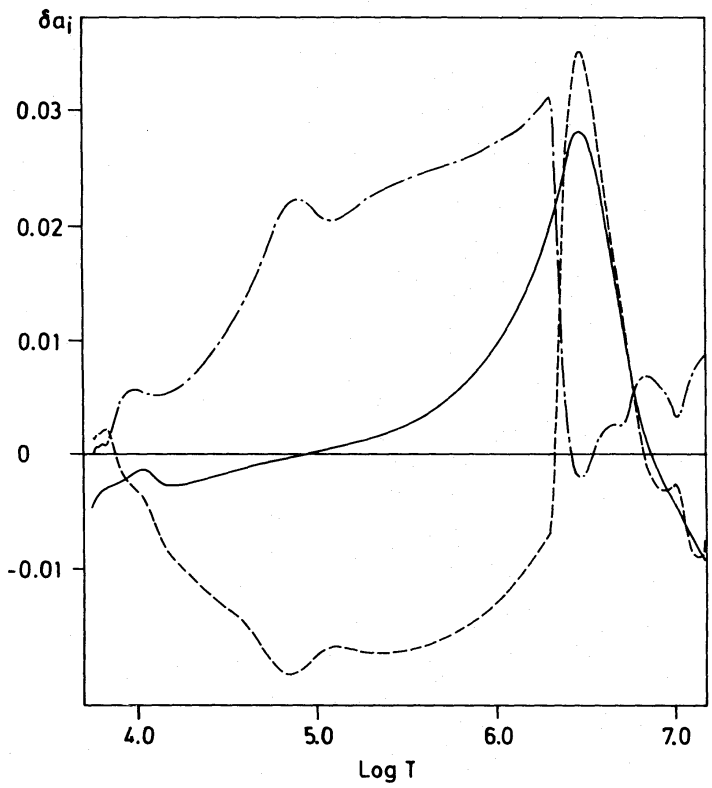

Figure 2. Differences between models 3 and 1 (*cf.* the caption to Fig. 1).

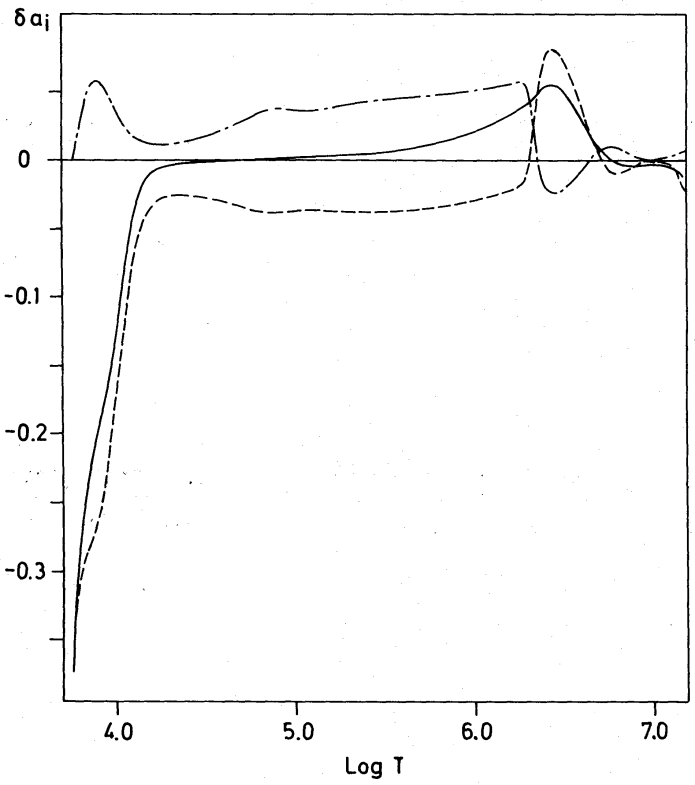

Figure 3. Differences between models 4 and 1 (*cf.* the caption to Fig. 1).

low temperatures are significantly larger than those of Cox & Tabor (*cf.* Christensen-Dalsgaard 1977), due probably to the partial neglect of absorption by molecules in the latter tables. In the interior of the model the differences are much smaller; the difference in surface values is compensated, in the calibration to the correct radius, by a considerable change in α, and the large differences in p and ρ are confined to the atmosphere and the very thin region near the top of the convection zone having an appreciable superadiabatic gradient (*cf.* Gough & Weiss 1976). Nevertheless there are significant differences in the interior of the model. Around the bottom of the convection zone the Carson opacity is smaller than that of Cox & Tabor, leading to a somewhat shallower convection zone in model 4. Close to the centre the Carson opacity is the larger, and consequently the central temperature and neutrino capture rate are higher in model 4 than in model 1; a similar effect was found by Carson, Ezer & Stothers (1974).

5 Oscillation periods

We have calculated a selection of linear, adiabatic modes of oscillation for each of the five models of the present Sun described in Table 1. The outer mechanical boundary condition on the oscillations was based on the solution to the adiabatic wave equation in an isothermal atmosphere (in the manner of, for example, Unno *et al.* 1979), and was applied at $\tau = 10^{-4}$ in the model atmosphere used to determine the outer boundary condition in the model calculation (*cf.* Section 2). Otherwise the calculation was as in Christensen-Dalsgaard (1980a), using a second-order centred difference scheme to integrate the equations of oscillation. Improved estimates of the frequencies of oscillation were obtained by substituting the eigenfrequencies into a variational expression, using the procedure of Christensen-Dalsgaard, Gough & Morgan (1979) for acoustic modes and a slight modification of it for gravity modes; these procedures are discussed in Appendix D.

The resulting periods of oscillation are presented in Table 3. Beside the fundamental radial mode ($p_1(l = 0)$) and $g_1(l = 1)$ the modes computed correspond to periods of oscillation determined observationally with high accuracy. These comprise the 5 min oscillations of low degree (Claverie *et al.* 1979, 1980; Grec *et al.* 1980) and the 160 min oscillation (e.g. Severny, Kotov & Tsap 1976, 1978; Kotov *et al.* 1978; Scherrer *et al.* 1979, 1980). In the latter case the modes chosen are those with periods closest to 160 min in models 1–3; in model 4 $g_9(l = 2)$ and $g_{13}(l = 3)$ (with periods of 154.43 and 155.32 min, respectively) are closer.

The low-order modes (i.e. $p_1(l = 0)$ and $g_1(l = 1)$) were computed on the mesh used in the model calculation. This was insufficient to resolve adequately the rapid spatial oscillations of the high-order p and g modes. For these modes we used meshes with 600 points,

Table 3. Periods, in minutes, of selected modes of oscillation in the models presented in Table 1. The labelling of modes with $l > 0$ uses the Eckart classification (e.g. Scuflaire 1974), whereas the labeling of radial modes follows Christensen-Dalsgaard *et al.* (1979).

Mode	Model 1	Model 1a	Model 2	Model 3	Model 4
$p_{29}(l = 0)$	4.0366	4.0357	4.0407	4.0404	4.0540
$p_{17}(l = 0)$	6.6922	6.6906	6.6996	6.6995	6.7148
$p_{28}(l = 1)$	4.1087	4.1078	4.1125	4.1125	4.1265
$p_{16}(l = 1)$	6.8948	6.8935	6.8998	6.9023	6.9175
$p_1(l = 0)$	64.092	64.080	64.068	63.735	63.257
$g_1(l = 1)$	63.531	63.556	63.493	63.695	64.990
$g_5(l = 1)$	154.99	155.05	154.93	155.31	157.66
$g_{10}(l = 2)$	165.20	165.28	165.14	165.41	168.26
$g_{14}(l = 3)$	162.57	162.64	162.50	162.66	165.31

distributed largely on the basis of the asymptotic behaviour of p or g modes of high order (*cf.* Christensen-Dalsgaard 1977). The equilibrium model was transferred to the new meshes using four point Lagrangian interpolation.

A comparison of the results for models 1 and 2 shows that the contribution to the relative error in the periods of high order p modes in model 1 coming from the spatial truncation error in the model calculation is probably smaller than 1.5×10^{-3}; for low-order modes and the high-order g modes this contribution is about 6×10^{-4} or less. As this part of the error is expected to vary as $(N-1)^{-2}$, N being the number of points in the model calculation, the corresponding errors for model 2 can be estimated as about 4×10^{-4} and 1.5×10^{-4}, respectively.

Similarly, comparison of models 1 and 1a shows that truncation error in time in the calculation of the model changes the high-order p mode periods by about 2×10^{-4}; this however can be attributed almost entirely to the change in radius and so would largely be eliminated in a calibrated model with higher time resolution. On the other hand the contribution to the error in the g mode periods, when corrected for the radius change, is about 9×10^{-4}. This difference in sensitivity between p and g modes reflects the fact that the truncation error in time affects the structure of the model through the composition. In a calibrated model the resulting readjustment of the envelope structure, and hence the change in p mode periods, would largely be eliminated, whereas the change in the behaviour in the interior of the model of the buoyancy frequency, which strongly affects the g mode periods, would remain.

An upper bound on the total error in the periods, given the physics used in the model calculation and the assumption of adiabatic oscillations, can be estimated by adding to the sum of the two contributions discussed above the error in the oscillation calculation for a given model; this is estimated in Appendix D to be about 2×10^{-4} for the high-order p modes and 5×10^{-6} for the high-order g modes. Thus the total relative errors for the p and g modes computed in model 1 are probably less than 1.7×10^{-3} and 1.5×10^{-3}, respectively; for the modes in model 2 the corresponding values are 6×10^{-4} and 1.1×10^{-3}.

The effect on the periods of the opacity interpolation can be seen by comparing models 1 and 3. For the high-order p modes the effect is small, due probably to the relatively small differences between the models near the surface (*cf.* Fig. 2). Less easy to understand is the fact that the largest difference, about 6×10^{-3}, is found for the $p_1(l = 0)$ mode, which *a priori* might be expected to be rather insensitive to conditions near the bottom of the convection zone where the differences between the models are greatest. The differences for the g modes are significantly smaller, around or less than 2×10^{-3}.

In contrast substantial differences are found between models 1 and 4, indicating that the periods are sensitive to the choice of opacity tables. Thus the differences between the periods of the high-order p modes, around 0.4 per cent, are considerably larger than their expected errors; the differences of 1–2 per cent in the periods of the fundamental radial and the g modes presumably reflect the rather large differences in the interior of the models, shown on Fig. 3.

Some quantities related to the overall properties of the 5 min oscillations of low degree are presented in Table 4. These are the mean frequency separations over the range considered

$$\overline{\Delta\nu}(l) = (\nu_{n_2,l} - \nu_{n_1,l})/(n_2 - n_1), \tag{5.1}$$

and the mean splitting between the almost degenerate frequencies of modes whose degrees differ by 2 (e.g. Christensen-Dalsgaard & Gough 1980a, b):

$$\overline{\delta\nu}(l) = \tfrac{1}{2}(\nu_{n_1,l} - \nu_{n_1-1,l+2} + \nu_{n_2,l} - \nu_{n_2-1,l+2}); \tag{5.2}$$

Table 4. Mean frequency separation $\overline{\Delta\nu}$ and mean frequency splitting $\overline{\delta\nu}$, defined by equations (5.1) and (5.2) respectively, in μHz.

	Model 1	Model 1a	Model 2	Model 3	Model 4
$\overline{\Delta\nu}(0)$	136.53	136.56	136.41	136.43	135.76
$\overline{\Delta\nu}(1)$	136.61	136.64	136.43	136.50	135.79
$\overline{\delta\nu}(0)$	10.3	10.2	9.6	10.3	10.6
$\overline{\delta\nu}(1)$	15.6	15.6	15.6	15.7	15.9

here $\nu_{n,l'}$ denotes the cyclic frequency of the mode $p_n(l = l')$, and the range (n_1, n_2) in order is the same as for the modes presented in Table 3. The variation in $\overline{\Delta\nu}$ between the models follows closely the behaviour of the frequencies discussed above. Thus the contribution to the relative error in $\overline{\Delta\nu}$ coming from the truncation error in the equilibrium model is estimated to be around 1.5×10^{-3} in model 1; the opacity interpolation has little effect on $\overline{\Delta\nu}$, whereas there is a significant relative difference, about 6×10^{-3}, between the values for models 1 and 4. On the other hand $\overline{\delta\nu}(0)$ is apparently rather sensitive to errors in the model; this is probably caused by the fact that the perturbation in the gravitational potential, for radial oscillations, is eliminated analytically using the equations of stellar structure. The error in $\overline{\delta\nu}(1)$, which is not as directly affected by errors in the model, and the changes in $\overline{\delta\nu}$ caused by changing the opacity interpolation or opacity tables, are all relatively small.

6 Discussion

The main purpose of the present study has been to investigate and reduce the extent to which numerical error affects models of the present Sun and the periods of oscillation computed for such models. Thus no attempt has been made to create a programme that is applicable to any type of star; in particular the programme does not provide for mixing in a convective core, and so it cannot be used to compute the evolution of stars more massive than the Sun.

This is no serious limitation, however. There already exists a number of general stellar evolution programmes, and these have been used for comprehensive calculations of stellar evolution over a wide range of parameters and model ages. Rather than competing with such comprehensive calculations the present work is aimed at complementing them by providing accurate models of the Sun. These are needed in helio-seismological investigations, where observed periods of solar oscillations are used to get information about the structure of the solar interior. This clearly requires that the errors in the calculation of the oscillations periods, given the physical assumptions made in the model calculation, be much smaller than the effects on the periods of changes in the model caused by reasonable modifications of these assumptions. A thorough investigation of the sensitivity of the periods to variations in the equilibrium model is outside the scope of the present work; however, as an example, we consider the effect of the treatment of the opacity.

6.1 ERRORS IN THE EQUILIBRIUM MODEL

These were estimated in Section 4 by comparing models computed on different spatial meshes or with different time steps. It was found that in a model (model 1) having 201 points and with 14 time steps covering the evolution until the present age of the Sun, the maximum contribution from spatial truncation to the relative error in pressure was about

2.3×10^{-2}, with smaller errors in temperature and density; the relative errors in the depth of the convection zone and the neutrino capture rate were about 10^{-3} and 2.5×10^{-3}, respectively. The corresponding contributions from truncation in time were all less than 10^{-3}. Thus the model is determined with reasonable accuracy with this choice of spatial mesh and time step.

6.2 ERRORS IN THE PERIODS

The errors in the computed periods arise partly from errors in the equilibrium model, partly from errors in the calculation of periods for a given model. In Appendix D it was shown that by using the variational principle for the frequency of adiabatic oscillation the latter errors could be reduced to below 2×10^{-4} for acoustic modes with periods in the vicinity of 5 min, and to less than 5×10^{-6} for gravity modes close to 160 min. The contributions from the errors in the equilibrium model were estimated in Section 5. It was found that for the acoustic modes the truncation error in space dominated, giving rise in model 1 to a relative error of about 1.5×10^{-3}; for gravity modes the spatial and temporal truncation caused comparable errors, the total relative error being again about 1.5×10^{-3} in model 1.

These values should clearly be compared with the errors in the observed periods, as well as with the sensitivity of the periods to changes in the model. Claverie *et al.* (1979, 1980) found that the relative error in the mean frequency separation for the 5 min modes was about 2×10^{-3}. A comparable error in the position of individual peaks can be inferred from the peak positions tabulated by Claverie *et al.* (1980) for four years of observation. Christensen-Dalsgaard & Gough (1982) analysed artificial data, assumed to be noise-free, that simulated the observations of Claverie *et al.* They found relative errors in the mean frequency separation, in averages of fairly large numbers of spectra, of about 10^{-3}; these errors were caused partly by interference between modes whose frequencies were too close to be resolved, partly by the departure from linearity in the relation between mode order and frequency. Thus it seems unlikely that this uncertainty can be considerably reduced in observations limited by the length of a day. In observations, made from the South Pole, that did not suffer from this limitation, Grec *et al.* (1980) found that the 5 min modes appeared to decay with an e-folding time of about two days. This would limit the relative accuracy in the determination of peak positions, in power spectra for continuous observations lasting considerably more than two days, to about 3×10^{-4}. The accuracy achieved by Grec *et al.* was in fact close to this limit. Finally the fact that the 160 min oscillation has apparently preserved its phase for at least six years (Scherrer *et al.* 1980) indicates that its period is now known with an accuracy of about 5×10^{-5}

As to the sensitivity of the periods to changes in the physics of the model, the results of Section 5 showed that changing the opacity tables from those of Cox & Tabor (1976) to those of Carson (1976) changed the acoustic mode periods by 0.3–0.4 per cent, and the mean frequency separations by about 0.6 per cent. These changes are significantly larger than the theoretical and observational errors discussed above; with the present accuracy it is therefore possible, on the basis of observations of the 5 min oscillations, to distinguish between those two sets of tables, provided no other changes in the model are considered. The changes in the gravity mode periods are very much larger than the errors, and so these modes are potentially more sensitive to changes in the opacity tables. Before this sensitivity can be utilized, however, an observational determination of the degree of the mode responsible for the 160 min oscillation must be made.

Further improvements in the accuracy of the computed periods, most urgently for the acoustic modes, are warranted by the precision of the observed periods. As discussed above

this mainly requires that the errors in the model computation be reduced. One immediate and significant reduction in the errors would result from using a model with 401 rather than 201 spatial mesh points. As the numerical integration scheme is of second order in space this would reduce the errors in the model by roughly a factor of 4; thus the errors in the acoustic mode periods for model 2, given in Table 3, are probably less than 6×10^{-4}. To reduce the errors even further one might use a higher order integration scheme, such as the fourth order scheme presented by Cash & Moore (1980) or the very similar scheme of Scuflaire (1980). Preliminary calculations, using the method of Cash & Moore, of static, chemically homogeneous models showed that these could be computed with a maximum relative error in p, ρ and T of about 10^{-3}, on a mesh with 201 points and a distribution that was inferior to that used in the present calculation. A fourth order scheme could also be used in the calculation of the oscillations and might eliminate the need for using the variational method to calculate improved periods.

6.3 COMPARISON WITH OTHER MODELS

The depths of the convection zones in the present solar models, described in Table 1, are somewhat greater than the depths quoted for other recent published solar models. Thus Gough & Weiss (1976) found $D/r_s = 0.22$ in a model with $Z = 0.02$; and the 'standard' model of Christensen-Dalsgaard *et al.* (1979), which differed from the model of Gough & Weiss in the use of improved nuclear reaction rates, had $D/r_s = 0.24$. Both calculations used Eggleton's (1971) programme and Cox & Stewart (1970) opacities with linear interpolation. In contrast the models computed here with Cox & Tabor (1976) opacities have $D/r_s = 0.27$–0.28; use of Cox & Stewart opacities gives very similar results (*cf.* Christensen-Dalsgaard 1977). A possible explanation for this discrepancy is the rather poor numerical resolution in the Eggleton programme near the base of the convection zone (Christensen-Dalsgaard *et al.* 1974).

The properties of the convection zone affects two observable characteristics of the Sun, viz. the depletion of the surface Li abundance relative to the cosmological value (e.g. Weymann & Sears 1965) and the frequencies of the 5 min modes of high degree (Gough 1977a; Rhodes *et al.* 1977). The rate of Li depletion is controlled by the temperature T_B at the bottom of the convection zone; in all models computed here this is significantly smaller than the value of about 2.6×10^6 K where the e-folding time of ^{7}Li is comparable with the age of the Sun (Straus, Blake & Schramm 1976), although slightly larger in model 1 than the value of 2.0×10^6 K quoted by Straus *et al.*

The frequencies of the 5 min modes of high degree are largely determined by the relation between p and ρ in the adiabatic part of the convection zone (Gough 1977a; Ulrich & Rhodes 1977). This can conveniently be expressed in terms of the value of $K \equiv p/\rho^{\Gamma_1}$, where $\Gamma_1 = (\partial \ln p/\partial \ln \rho)_s$ (s being specific entropy), as this quantity is approximately constant in the adiabatic part of the convection zone, beneath the ionization zones of H and He. For given chemical composition K is closely related to the depth of the convection zone. Berthomieu *et al.* (1980) obtained almost perfect agreement between observed and calculated frequencies with an envelope model having $K = 5.5 \times 10^{14}$ (in cgs units) at a depth of 1.5×10^5 km, and with $D/r_s = 0.33$. For comparison the value of K at the same depth in model 1 is 9.4×10^{14}. To increase K to the value of Berthomieu *et al.* would require increasing the efficacy of convection in the superadiabatic boundary layer near the top of the convection zone, to reduce the temperature gradient in this region (within the framework of mixing length theory this corresponds to increasing the mixing length), but the convection zone would then no longer fit the interior of the model. Whether this discrepancy represents a serious difficulty remains to be seen.

The neutrino capture rates found here are in reasonable agreement with previous results (e.g. Bahcall 1977). It should be noticed, however, that improvements in the opacity calculation since the computation of the Cox & Tabor (1976) tables lead to an increase in the capture rate (Bahcall *et al.* 1980).

6.4 SHORTCOMINGS OF THE CALCULATION

To allow fairly extensive analysis of the numerical accuracy a number of simplifying assumptions has been made in the present model calculation. The assumption of a static, chemically homogeneous initial model, as well as the assumed nuclear equilibrium of the CN cycle, may have some effect on the early evolution of the model. To investigate the importance of the latter assumption we have integrated the equations for the full CNO tri-cycle (Rolfs & Rodney 1974) in time at selected mass points in models belonging to an evolution sequence similar to sequence 1 of Table 1. The initial burning of ^{12}C releases energy at a rate that at the centre reaches a maximum value of about 30 per cent of the energy generation rate ϵ_{PP} of the PP chains. In this stage the model would almost certainly have a convective core. On the other hand this phase is relatively shortlived; after about 10^8 yr of evolution the energy generation rate from non-equilibrium CN reactions is less than 10 per cent of ϵ_{PP} everywhere in the model, and at an age of 10^9 yr the CN cycle is in equilibrium in all parts of the model where CN energy generation is significant. The reactions involving ^{16}O proceed so slowly that only about 3 per cent of the initial ^{16}O abundance has been consumed at the centre of the model by the time it reaches the present age of the Sun. Thus the ^{16}O branch of the cycle can justifiably be neglected in calculations of solar models. The reactions in the CN cycle should clearly be included in calculations of early evolutionary stages. But here the pre-main sequence history of the model also has an important effect on the chemical composition (Iben 1965), and the contraction to the main sequence should be properly calculated. During the time taken for the CN cycle to reach equilibrium X is only reduced by roughly 1 per cent, however; thus models of the present Sun are probably only slightly affected by the assumption of CN equilibrium. Nevertheless the resulting modification in the behaviour of the hydrogen abundance may have a small effect on the g mode periods.

Somewhat more important, for the acoustic mode periods at least, is the use of an approximate treatment of the equation of state. The calculations of Berthomieu *et al.* (1980) and Lubow *et al.* (1980) showed that the inclusion of non-ideal effects in the equation of state had a noticeable effect on the periods of the 5 min modes with high l; similar effects, of the order of 0.1 per cent, may also be expected for 5 min modes of low degree. The opacity should also be improved. The results found in Sections 4 and 5 showed that the use of linear interpolation in opacity, while unimportant for the acoustic modes, causes significant changes in the depth of the convection zone and the neutrino flux of the model as well as in the gravity mode periods. This strongly suggests a need for opacity tables with a finer grid at the temperatures and densities found in the interior of the model. In addition the tables should have the observed (e.g. Ross & Aller 1976) ratios between the heavy element and the hydrogen abundances. Finally the assumed solar luminosity may be slightly too low; thus very recent results from the Solar Maximum Mission (Willson *et al.* 1981) give a mean luminosity of 3.8481×10^{33} erg s^{-1}.

The pulsation calculation also needs improvements, in particular for the high-order acoustic modes. The frequencies of these modes are relatively sensitive to the behaviour of the eigenfunction close to the outer boundary of the model (Christensen-Dalsgaard & Gough 1980b), where the oscillations are not adiabatic; thus non-adiabatic effects may be expected

to have a significant influence on the periods, and the calculation should be based on the full non-adiabatic equations. For these modes the perturbations of the turbulent Reynolds stresses in the convection zone may possibly also affect the periods; thus turbulent pressure should be taken into account in the calculation of the equilibrium model (this has yet to be done in a consistent fashion), and the computation of the oscillations should include a model for the Reynold's stress perturbation (e.g. Gough 1977b). The low-order acoustic modes and the gravity modes are much less sensitive to conditions in the outer part of the model, and so for these modes the present adiabatic treatment is probably adequate.

6.5 COMPARISON OF OBSERVED AND CALCULATED PERIODS

Because of the deficiencies, discussed above, in the present calculation a detailed comparison between calculated and observed periods for the 5 min oscillations of low degree is somewhat premature. Average properties of the spectrum are probably less sensitive to these problems, however, and may be used for an initial comparison. As pointed out by Christensen-Dalsgaard & Gough (1980b) the discrepancies between theory and observation for the mean frequency separation $\overline{\Delta\nu}$ appear to be within the variation possible among traditional solar models, whereas the observed values of $\overline{\Delta\nu}$ are inconsistent with the non-standard models B and C, with low initial abundances of heavy elements, of Christensen-Dalsgaard *et al.* (1979). The mean splittings $\overline{\delta\nu}(l)$ between $\nu_{n,l}$ and $\nu_{n-1,l+2}$, for $l = 0$ and 1, were measured by Grec *et al.* (1980) as 10 and 16 μHz, respectively. The theoretical results in Table 4 are in excellent agreement with these values; these results furthermore show that $\overline{\delta\nu}$ is insensitive to changes in the opacity tables. On the other hand $\overline{\delta\nu}$ is sensitive to more drastic modifications of the model. Thus Christensen-Dalsgaard & Gough (1980b) showed that a decrease in the interior heavy element abundances led to a significant increase in $\overline{\delta\nu}$. Furthermore, a chemically homogeneous, static model with the same physics as model 1 of Table 1, calibrated to have solar radius and luminosity, was found to have $\overline{\delta\nu}(0) = 15\,\mu$Hz and $\overline{\delta\nu}(1) = 22\,\mu$Hz, which is clearly inconsistent with the observations; this result is particularly interesting because the chemically homogeneous model cannot be distinguished from model 1 on the basis of $\overline{\Delta\nu}$ (*cf.* Christensen-Dalsgaard & Gough 1980b).

The periods computed for the modes close to 160 min are probably less affected by the deficiencies in the calculation, but here a definite comparison between observed and theoretical periods has to await a determination of the degree of the mode responsible for the 160 min oscillation. The ratio between the amplitudes observed at Stanford and Crimea (Scherrer *et al.* 1980) is consistent with a degree of 3 (Christensen-Dalsgaard 1980b); Table 3 shows that the correct period for this value of l could be obtained by an opacity change of the same magnitude as the change from the Cox & Tabor (1976) to the Carson (1976) tables, but of opposite sign. However, these modes are also sensitive to the variations in chemical composition in the interior of the model; thus in the chemically homogeneous model mentioned above the mode of degree 3 closest to 160 min is g_6, with a period of 152.8 min. Thus even a modest degree of mixing of the solar interior (e.g. Dilke & Gough 1972; Schatzman & Maeder 1980, 1981) would change the gravity mode periods significantly. Clearly a definite identification of other modes in this period range, together with a determination of their degree, would be of great value in helping to discriminate between these possibilities.

7 Conclusions

A more systematic investigation than has been attempted here of the sensitivity of oscillation periods to changes in the equilibrium model is needed before the potentials for

helio-seismology can be fully assessed. Nevertheless our results show that the observational and computational accuracy is such that the observed periods put fairly stringent constraints on the interior structure of solar models. The problems encountered in attempts to meet the so far only other constraint, the neutrino capture rate, suggest that the construction of models satisfying these new constraints may prove difficult.

Acknowledgments

I am deeply indebted to D. O. Gough for his assistance on this project. We developed the programme used to solve the non-linear partial differential equations in collaboration, and he has provided much guidance on other aspects of the work. I thank T. P. Caudell, E. Fossat, V. A. Kotov, D. R. Moore, H. Saio, R. Scuflaire, R. J. Tayler and N. O. Weiss for helpful conversations, and P. P. Eggleton for providing me with his copy of Carson's opacity tables. I am grateful to Professor P. Ledoux for hospitality at Institut d'Astrophysics, Liège, and to Professor M. J. Rees for hospitality at Institute of Astronomy, Cambridge, where much of the computation was completed. Financial support from Statens naturvidenskabelige Forskningsråd, Denmark, and from Aarhus Universitet is gratefully acknowledged.

References

Abraham, Z. & Iben, Jr, I., 1971. *Astrophys. J.*, **170**, 157.
Allen, C. W., 1973. *Astrophysical Quantities*, 3rd edn, Athlone Press, London.
Bahcall, J. N., 1977. *Astrophys. J.*, **216**, L115.
Bahcall, J. N., Bahcall, N. A. & Ulrich, R. K., 1969. *Astrophys. J.*, **156**, 559.
Bahcall, J. N. & Davis, Jr, R., 1976. *Science*, **191**, 264.
Bahcall, J. N., Huebner, W. F., Magee, N. H., Merts, A. C. & Ulrich, R. K., 1973. *Astrophys. J.*, **184**, 1.
Bahcall, J. N., Lubow, S. H., Heubner, W. F., Magee, N. H., Merts, A. L., Argo, M. F., Parker, P. D., Roznyai, B. & Ulrich, R. K., 1980. *Phys. Rev. Lett.*, **45**, 945.
Baker, N. H., Moore, D. W. & Spiegel, E. A., 1971. *Q. J. Mech. Appl. Math.*, **24**, 391.
Baker, N. H. & Temesváry, S., 1966. *Tables of Convective Stellar Envelopes*, Goddard Institute for Space Studies, New York.
Barger, V., Whisnant, K. & Phillips, R. J. N., 1980. *Phys. Rev. D*, **22**, 1636.
Berthomieu, G., Cooper, A. J., Gough, D. O., Osaki, Y., Provost, J. & Rocca, A., 1980. *Lecture Notes in Physics*, **125**, 307, eds Dziembowski, W. & Hill, H. A., Springer, Heidelberg.
Böhm-Vitense, E., 1958. *Z. Astrophys.*, **46**, 108.
Brown, T. M., Stebbins, R. T. & Hill, H. A., 1978. *Astrophys. J.*, **223**, 324.
Carson, T. R., 1976. *A. Rev. Astr. Astrophys.*, **14**, 95.
Carson, T. R., Ezer, D. & Stothers, R., 1974. *Astrophys. J.*, **194**, 743.
Cash, J. R. & Moore, D. R., 1980. *BIT*, **20**, 1.
Caudell, T. P., Knapp, J., Hill, H. A. & Logan, J. D., 1980. *Lecture Notes in Physics*, **125**, 206, eds Dziembowski, W. & Hill, H. A., Springer, Heidelberg.
Chandrasekhar, S., 1964. *Astrophys. J.*, **139**, 664.
Christensen-Dalsgaard, J., 1977. *PhD dissertation*, University of Cambridge.
Christensen-Dalsgaard, J., 1980a. *Mon. Not. R. astr. Soc.*, **190**, 765.
Christensen-Dalsgaard, J., 1980b. *Proc. Vth European Regional Meeting in Astronomy*, Institute d'Astrophysique, Liège.
Christensen-Dalsgaard, J., 1981. *Mon. Not. R. astr. Soc.*, **194**, 229.
Christensen-Dalsgaard, J., Dilke, F. W. W. & Gough, D. O., 1974. *Mon. Not. R. astr. Soc.*, **169**, 429.
Christensen-Dalsgaard, J. & Gough, D. O., 1976. *Nature*, **259**, 89.
Christensen-Dalsgaard, J. & Gough, D. O., 1980a. *Lecture Notes in Physics*, **125**, 184, eds Dziembowski, W. & Hill, H. A., Springer, Heidelberg.
Christensen-Dalsgaard, J. & Gough, D. O., 1980b. *Nature*, **288**, 544.
Christensen-Dalsgaard, J. & Gough, D. O., 1982. *Mon. Not. R. astr. Soc.*, **198**, 141.
Christensen-Dalsgaard, J., Gough, D. O. & Morgan, J. G., 1979. *Astr. Astrophys.*, **73**, 121.
Claverie, A., Isaak, G. R., McLeod, C. P., van der Raay, H. B. & Roca Cortes, T., 1979. *Nature*, **282**, 591.

Claverie, A., Isaak, G. R., McLeod, C. P., van der Raay, H. B. & Roca Cortes, T., 1980. *Astr. Astrophys.*, **91**, L9.
Clayton, D. D., 1968. *Principles of Stellar Evolution and Nucleosynthesis,* McGraw-Hill, New York.
Cline, A. K., 1974. *Comm. ACM,* **17**, 218.
Cox, A. N. & Stewart, J. N., 1970. *Astrophys. J. Suppl.*, **19**, 243.
Cox, A. N. & Tabor, J. E., 1976. *Astrophys. J. Suppl.*, **31**, 271.
Cox, J. P., 1980. *Theory of Stellar Pulsation,* Princeton University Press, Princeton, NJ.
Deubner, F.-L., 1975. *Astr. Astrophys.*, **44**, 371.
Deubner, F.-L., Ulrich, R. K. & Rhodes, Jr, E. J., 1979. *Astr. Astrophys.*, **72**, 177.
Dilke, F. W. W. & Gough, D. O., 1972. *Nature,* **240**, 262.
Eggleton, P. P., 1971. *Mon. Not. R. astr. Soc.*, **151**, 351.
Eggleton, P. P., 1972. *Mon. Not. R. astr. Soc.*, **156**, 361.
Eggleton, P. P., Faulkner, J. & Flannery, B. P., 1973. *Astr. Astrophys.*, **23**, 325.
Fowler, W. A., Caughlan, G. R. & Zimmerman, B. A., 1975. *A. Rev. Astr. Astrophys.*, **13**, 69.
Gingerich, O., Noyes, R. W., Kalkofen, W. & Cuny, Y., 1971. *Solar Phys.*, **18**, 347.
Gough, D. O., 1977a. *Proc. IAU Colloq. No. 36,* p. 3, eds Bonnet, R. M. & Delache, Ph., G. de Bussac, Clermont-Ferrand.
Gough, D. O., 1977b. *Astrophys. J.*, **214**, 196.
Gough, D. O., Spiegel, E. A. & Toomre, J., 1975. *Lecture Notes in Physics,* **35**, 191, ed. Richtmyer, R. D., Springer, Heidelberg.
Gough, D. O. & Weiss, N. O., 1976. *Mon. Not. R. astr. Soc.*, **176**, 589.
Grec, G., Fossat, E. & Pomerantz, M., 1980. *Nature,* **288**, 541.
Henyey, L. G., Wilets, L., Böhm, K. H., LeLevier, R. & Levée, R. D., 1959. *Astrophys. J.*, **129**, 628.
Hill, H. A. & Stebbins, R. T., 1975. *Astrophys. J.*, **200**, 471.
Iben, Jr, I., 1965. *Astrophys. J.*, **141**, 993.
Iben, Jr, I., Kalata, K. & Schwartz, J., 1967. *Astrophys. J.*, **150**, 1001.
Kotov, V. A., Severny, A. B. & Tsap, T. T., 1978. *Mon. Not. R. astr. Soc.*, **183**, 61.
Ledoux, P. & Pekeris, C. L., 1941. *Astrophys. J.*, **94**, 124.
Ledoux, P. & Walraven, T., 1958. *Handbuch der Physik,* vol. 51, chapter IV, Springer-Verlag, Berlin.
Lubow, S. H., Rhodes, Jr, E. J. & Ulrich, R. K., 1980. *Lecture Notes in Physics,* **125**, 300, eds Dziembowski, W. & Hill, H. A. Springer, Heidelberg.
Pekeris, C. L., 1938. *Astrophys. J.*, **88**, 189.
Reines, F., Sobel, H. W. & Pasierb, E., 1980. *Phys. Rev. Lett.*, **45**, 1307.
Rhodes, Jr, E. J., Ulrich, R. K. & Simon, G. W., 1977. *Astrophys. J.*, **218**, 901.
Rolfs, C. & Rodney, W. S., 1974. *Astrophys. J.*, **194**, L63.
Ross, J. E. & Aller, L. H., 1976. *Science,* **191**, 1223.
Salpeter, E. E., 1954. *Aust. J. Phys.*, **7**, 373.
Schatzman, E. & Maeder, A., 1980. *C. r. Acad. Sci. Paris, Serié B,* **291**, 81.
Schatzman, E. & Maeder, A., 1981. *Astr. Astrophys.*, **96**, 1.
Scherrer, P. H., Wilcox, J. M., Kotov, V. A., Severny, A. B. & Tsap, T. T., 1979. *Nature,* **277**, 635.
Scherrer, P. H., Wilcox, J. M., Severny, A. B., Kotov, V. A. & Tsap, T. T., 1980. *Astrophys. J.*, **237**, L97.
Scuflaire, R., 1974. *Astr. Astrophys.*, **36**, 107.
Scuflaire, R., 1980. Preprint.
Scuflaire, R., Gabriel, M., Noels, A., Boury, A., 1975. *Astr. Astrophys.*, **45**, 15.
Severny, A. B., Kotov, V. A. & Tsap, T. T., 1976. *Nature,* **259**, 87.
Severny, A. B., Kotov, V. A. & Tsap, T. T., 1978. *Pleins feux sur la physique solaire,* p. 123, ed. Rösch, J., CNRS, Paris.
Straus, J. M., Blake, J. B. & Schramm, D. M., 1976. *Astrophys. J.*, **204**, 481.
Ulrich, R. K. & Rhodes, Jr, E. J., 1977. *Astrophys. J.*, **218**, 521.
Unno, W., Osaki, Y., Ando, H. & Shibahashi, H., 1979. *Nonradial Oscillations of Stars,* University of Tokyo Press.
Weymann, R. & Sears, R. L., 1965. *Astrophys. J.*, **142**, 174.
Willson, R. C., Gulkis, S., Janssen, M., Hudson, H. S. & Chapman, G. A., 1981. *Science,* **211**, 700.

Appendix A: The central boundary condition

It may be shown (e.g. Christensen-Dalsgaard *et al.* 1974) that the first derivatives with respect to r of p, T, X and X_3 vanish at the centre. Thus any thermodynamic function, for

instance the density ρ, may be expanded as

$$\rho(r) = \rho_c + \tfrac{1}{2}\rho_2 r^2 + \ldots, \tag{A1}$$

where ρ_c is the central value of ρ and

$$\rho_2 = \left(\frac{\partial\rho}{\partial r}\right)_{T,X} p_2 + \left(\frac{\partial\rho}{\partial T}\right)_{p,x} T_2 + \left(\frac{\partial\rho}{\partial X}\right)_{p,T} X_2; \tag{A2}$$

here p_2, T_2 and X_2 are central values of the second derivatives of p, T and X.

From equation (A1) and the mass equation follows that

$$m(r) = \tfrac{4}{3}\pi r^3(\rho_c + \tfrac{3}{10}\rho_2 r^2 + \ldots), \tag{A3}$$

and hence, using the equation of hydrostatic support

$$p(r) = p_2 - \tfrac{2}{3}\pi\rho_c^2 r^2 - \tfrac{4}{15}\pi\rho_c\rho_2 r^4 + \ldots. \tag{A4}$$

The expansion of the luminosity requires a little more care. Introducing the variables $v^{(\mu)}$, $\mu = 1,\ldots,4$, by $v^{(1)} = p$, $v^{(2)} = T$, $v^{(3)} = X$ and $v^{(4)} = X_3$, we may write the energy equation as

$$\frac{\partial L}{\partial r} = 4\pi\rho r^2\left[\epsilon - \sum_{\mu=1}^{3} S_\mu\left(\frac{\partial v^{(\mu)}}{\partial t}\right)_m\right], \tag{A5}$$

where ϵ is the nuclear energy generation rate per unit mass, and

$$S_1 = \left(\frac{\partial H}{\partial p}\right)_{T,X} - \frac{1}{\rho}, \quad S_2 = \left(\frac{\partial H}{\partial T}\right)_{p,X}, \quad S_3 = \left(\frac{\partial H}{\partial X}\right)_{p,T}, \tag{A6}$$

H being the enthalpy per unit mass. Taking into account the change from time derivatives at constant m to time derivatives at constant r equation (A5) implies that

$$L(r) = \mathscr{L}_0 r^3 + \mathscr{L}_2 r^5, \tag{A7}$$

where

$$\mathscr{L}_0 = \frac{4\pi\rho_c}{3}\left[\epsilon_c - \sum_{\mu=1}^{3} S_{\mu,c}\frac{dv_c^{(\mu)}}{dt}\right] \tag{A8}$$

and

$$\mathscr{L}_2 = \frac{2\pi}{5}\rho_2\left(\epsilon_c - S_{\mu,c}\frac{dv_c^{(\mu)}}{dt}\right) + \frac{2\pi}{5}\rho_c\left\{\epsilon_2 - \sum_{\mu=1}^{3}\left[S_{\mu,2}\frac{dv_c^{(\mu)}}{dt} + S_{\mu,c}\left(\frac{dv_2^{(\mu)}}{dt} - \frac{2}{3}v_2^{(\mu)}\frac{d\ln\rho_c}{dt}\right)\right]\right\}, \tag{A9}$$

here $v_c^{(\mu)}$ and $v_2^{(\mu)}$ are the central values of $v^{(\mu)}$ and $d^2v^{(\mu)}/dr^2$, ϵ_c and $S_{\mu,c}$ are central values of ϵ and S_μ and the second derivatives ϵ_2 and $S_{\mu,2}$ of these quantities are determined by expressions similar to equation (A2).

The treatment of the time derivatives in equations (A8) and (A9), and in the discretization of the energy equation, must be consistent. Thus if t^s and t^{s+1} are two consecutive time

levels, the value $\mathscr{L}_0^{s+1}$ of $\mathscr{L}_0$ at t^{s+1} is found from

$$\theta_4\mathscr{L}_0^{s+1} + (1-\theta_4)\mathscr{L}_0^{s} = \frac{4\pi}{3}\left\{\theta_4\rho_c^{s+1}\epsilon_c^{s+1} + (1-\theta_4)\rho_c^{s}\epsilon_c^{s} - \sum_{\mu=1}^{3}[\theta_4\rho_c^{s+1}S_{\mu,c}^{s+1} + (1-\theta_4)\rho_c^{s}S_{\mu,c}^{s}] \times (v_c^{(\mu),s+1} - v_c^{(\mu),s})/(t^{s+1}-t^{s})\right\}; \quad \text{(A10)}$$

here superscripts s and s+1 refer to values at t^s and t^{s+1}, respectively, and θ_4 is the centralization coefficient introduced in the discretization of the energy equation (*cf.* equation B7). $\mathscr{L}_2$ is treated similarly.

If the model has a radiative core (as in all cases considered here), the expansion of T follows from the expansion of L, using the equation for the radiative flux, as

$$T(r) = T_c - \frac{3\kappa_c\rho_c}{32\pi acT_c^3}\mathscr{L}_0 r^2 + \ldots, \quad \text{(A11a)}$$

where $\mathscr{L}_0$ is found from equation (A10); here κ_c is the central value of the opacity, a is the radiation density constant and c the speed of light. In a convective core the temperature gradient is very nearly adiabatic, and so from equation (A4)

$$T(r) = T_c - \tfrac{2}{3}\pi\frac{T_c}{p_c}\rho_c^2\nabla_{ad,c}r^2 + \ldots, \quad \text{(A11b)}$$

where $\nabla_{ad} = (\partial \ln T/\partial \ln p)_s$, s being the specific entropy.

Finally we must consider the expansions of X and X_3. In a convective core the chemical composition is homogeneous, and the second derivatives of X and X_3 vanish. If the core is radiative we must use the rate equations which for X may be written

$$\left(\frac{\partial X}{\partial t}\right)_m = R_X, \quad \text{(A12)}$$

where R_X is a function of p, T, X and X_3. Changing again to time derivative at constant r and introducing $R^{(3)} = R_X$ and $R^{(4)} = R_{X_3}$ (the rate of change of X_3) equation (A12) and the corresponding equation for X_3 give

$$\frac{dv_2^{(\nu)}}{dt} = \frac{2}{3}\frac{d\ln\rho_c}{dt}v_2^{(\mu)} + R_2^{(\nu)}, \quad \nu = 3, 4, \quad \text{(A13)}$$

where $R_2^{(\nu)}$ is the second derivative of $R^{(\nu)}$ at the centre, and may be expressed in terms of $v_2^{(\mu)}$, $\mu = 1, \ldots, 4$, as in equation (A2). The two equations (A13) are then discretized in time, using the same centralization coefficients as in the corresponding stellar evolution equations (*cf.* equation B8), to give two linear equations for $v_2^{(3)}$ and $v_2^{(4)}$ at the time level t^{s+1}, in terms of quantities at t^s as well as $v_2^{(1),s+1}$ and $v_2^{(2),s+1}$. These in turn are given by equations (A4) and (A11) in terms of the central values of p, T, X and X_3. By equating the expansions of these quantities, truncated after the term in r^2, to their values at the innermost mesh point x_1 we therefore get a set of non-linear equations for p_c, T_c, X_c and X_{3c}, as functions of quantities at x_1. Once these equations have been solved (this must be done numerically) the expansion of m and L (equations A3 and A7) provide the requisite boundary conditions.

Appendix B: The difference equations

The equations of stellar evolution are of the general form

$$\frac{\delta y_l}{\partial x} = f_l(z_i, x), \qquad l = 1, \ldots, I1, \tag{B1}$$

$$\frac{\partial y_p}{\partial x} = f_p(z_i, x) + \sum_{i=1}^{I} \Lambda_{pi}(z_j, x)\,\frac{\partial z_i}{\partial t}, \qquad p = I1 + 1, \ldots, I1 + I2, \tag{B2}$$

$$\frac{\partial y_u}{\partial t} = f_u(z_i, x), \qquad u = I1 + I2 + 1, \ldots, I, \tag{B3}$$

where $I = I1 + I2 + I3$; in the present case $I1 = 3, I2 = 1$ and $I3 = 2$, with the y_i as defined in Section 2. Following the discussion in that section we have introduced in the right hand sides of equations (B1)–(B3) a new set of dependent variables z_i, related to the y_i by a non-singular transformation. The independent variable x lies in the interval (x_1, x_2), and the solution satisfies boundary conditions at x_1 and x_2 of the form

$$g_\alpha[z_i(x_1)] = 0, \qquad \alpha = 1, \ldots, \mathrm{KA}, \tag{B4}$$

$$g_\beta[z_i(x_2)] = 0, \qquad \beta = \mathrm{KA} + 1, \ldots, \mathrm{KA} + \mathrm{KB} \tag{B5}$$

(with KA = KB = 2 in the present case).

We introduce the mesh $x_1 = x^1 < \ldots < x^n < \ldots < x^N = x_2$ in x and consider two time levels t^s and t^{s+1}. Equations (B1)–(B3) are replaced by the following difference equations:

$$y_l^{n+1,s+1} - y_l^{n,s+1} = \tfrac{1}{2}\Delta x^n (f_l^{n+1,s+1} + f_l^{n,s+1}), \qquad n = 1, \ldots, N-1;\ l = 1, \ldots, I1, \tag{B6}$$

$$\begin{aligned}
&\theta_p (y_p^{n+1,s+1} - y_p^{n,s+1}) + (1-\theta_p)(y_p^{n+1,s} - y_p^{n,s}) \\
&\quad = \tfrac{1}{2}\Delta x^n \{\theta_p (f_p^{n+1,s+1} + f_p^{n,s+1}) + (1-\theta_p)(f_p^{n+1,s} + f_p^{n,s}) \\
&\qquad + \sum_{i=1}^{I} [\theta_p \Lambda_{pi}^{n+1,s+1} + (1-\theta_p)\Lambda_{pi}^{n+1,s}](z_i^{n+1,s+1} - z_i^{n+1,s})/\Delta t^s \\
&\qquad + \sum_{i=1}^{I} [\theta_p \Lambda_{pi}^{n,s+1} + (1-\theta_p)\Lambda_{pi}^{n,s}](z_i^{n,s+1} - z_i^{n,s})/\Delta t^s\},
\end{aligned}$$

$$n = 1, \ldots, N-1; \qquad p = I1 + 1, \ldots, I1 + I2, \tag{B7}$$

and

$$\begin{aligned}
&y_u^{n,s+1} - y_u^{n,s} = \Delta t^s [\theta_u f_u^{n,s+1} + (1-\theta_u) f_u^{n,s}], \\
&\quad n = 1, \ldots, N; \qquad u = I1 + I2 + 1, \ldots, I.
\end{aligned} \tag{B8}$$

Here $z_i^{n,s} = z_i(x^n, t^s)$ and is related to $y_i^{n,s}$ by

$$y_i^{n,s} = y_i(z_j^{n,s}, x^n), \qquad n = 1, \ldots, N; \qquad i = 1, \ldots, I; \tag{B9}$$

a similar notation is used for $f_i^{n,s}$ and $\Lambda_{pi}^{n,s}$. Finally $\Delta x^n = x^{n+1} - x^n$ and $\Delta t^s = t^{s+1} - t^s$. Equations (B6) and (B7) are evidently centred in x; the coefficients θ_i have been introduced to permit the use of different degrees of centralization in t, $\theta_i = \frac{1}{2}$ corresponding to time

centred differences. As discussed in Section 3 stability required θ_4 (in the energy equation) and θ_6 (in the equation for X_3) to be 1, whereas θ_5 (in the equation for X) could be ½.

If the $z_i^{n,s}$ are known equations (B6)–(B9), together with the boundary conditions which now become

$$g_\alpha(z_i^{1,s+1}) = 0, \quad \alpha = 1, \ldots, \mathrm{KA} \tag{B10}$$

$$g_\beta(z_i^{N,s+1}) = 0, \quad \beta = \mathrm{KA}+1, \ldots, \mathrm{KA}+\mathrm{KB}, \tag{B11}$$

constitute $2 \times N \times I - I1 - I2 + \mathrm{KA} + \mathrm{KB}$ non-linear algebraic equations for the $2 \times N \times I$ unknowns $y_i^{n,s+1}$ and $z_i^{n,s+1}$, $i = 1, \ldots, I$; $n = 1, \ldots, N$. Thus we get the consistency condition

$$I1 + I2 = \mathrm{KA} + \mathrm{KB}. \tag{B12}$$

The equations are solved by Newton–Raphson iteration. Given trial values $\bar{z}_i^{n,s+1}$ equations (B6)–(B8) can be linearized in the corrections $\delta z_i^n = z_i^{n,s+1} - \bar{z}_i^{n,s+1}$, to give

$$\sum_{i=1}^{I} (A_{ai}^{n,s+1}\,\delta z_i^n + B_{ai}^{n,s+1}\,\delta z_i^{n+1}) + D_a^{n,s+1} = 0, \quad n = 1, \ldots, N-1; \quad a = 1, \ldots, I1+I2, \tag{B13}$$

$$\sum_{i=1}^{I} \mathscr{A}_{ui}^{n,s+1}\,\delta z_i^n + \mathscr{D}_u^{n,s+1} = 0, \quad n = 1, \ldots, N, \quad u = I1+I2+1, \ldots, I; \tag{B14}$$

the coefficients in these equations are rather complicated and will not be presented here (see Christensen-Dalsgaard 1977). The linearization of (B10) and (B11) is obvious.

From (B14) δz_u^n, $u = I1+I2+1, \ldots, I$, can be expressed in terms of δz_a^n, $a = 1, \ldots, I1+I2$, provided the matrix

$$\{\mathscr{A}_{uv}^{n,s+1}\}_{u,v = I1+I2+1, \ldots, I}$$

is non-singular. Equation (B13) and the linearized boundary conditions can then be solved for the δz_a^n as usual (see, e.g. Baker, Moore and Spiegel, 1971) by forwards elimination and back substitution. It was found that to ensure convergence the elimination had to start at the surface. To improve the rate of convergence the derivatives with respect to z_i of the right-hand sides of the equations and the boundary conditions were evaluated analytically; the trial model was found by linear extrapolation from the previous two time levels, and only two to three iterations were in general needed for convergence to a mean correction smaller than 10^{-6}.

Appendix C: The mesh and the time step

In the spirit of the first derivative stretching introduced by Gough *et al.* (1975) the mesh is determined as being uniform in ξ, satisfying the differential equation

$$\frac{d\xi}{dx} = \lambda F \tag{C1}$$

here F is a functional of the solution $y_i(x, t^s)$, and λ is a parameter relating the ranges of ξ and x. In the present case the following choice of F was found to be suitable:

$$F = \left\{ \sum_{i=1}^{6} w_i^2 S_i^{-2} \left(\frac{\partial \eta_i}{\partial x}\right)^2 + w_7^2 S_7^{-2} \left[\left(\frac{\partial \eta_7}{\partial x}\right)^2 + a_7^2 \eta_7^2 \left(\frac{\partial^2 \eta_7}{\partial x^2}\right)^2 \right] + w_8^2/(x_2 - x_1)^2 \right\}^{-1/2}. \tag{C2}$$

Here $\eta_1 = r$, $\eta_2 = \log p$, $\eta_3 = \log T$, $\eta_4 = \log L$, $\eta_5 = R_X$, $\eta_6 = \log(10^{-5} + X_3)$ and $\eta_7 = \nabla - \nabla_{ad}$, where $\nabla = d \log T/d \log p$; (x_1, x_2) is the interval in x, s_i is the range of η_i and the w_i's are adjustable weight factors. In the calculation we use $w_1 = w_2 = w_3 = 3$, $w_4 = w_5 = w_7 = w_8 = 1$ and $w_6 = 0.3$; furthermore a_7 is 10^{-11}, i.e. comparable with the distance in x from the surface to the maximum in $\nabla - \nabla_{ad}$. The sensitivity of the model to changes in w_1 and w_7 is analysed in Christensen-Dalsgaard (1977).

It is possible to regard equation (C1) as a differential equation for x which is solved together with the equations of stellar structure, using ξ as the independent variable. However we use the simpler approach of evaluating F with a solution $y_i(x, t^s)$ found on a trial mesh; solving equation (C1) then clearly reduces to quadrature. The solution is transferred to the new mesh using four point Lagrangian interpolation. For the initial model the equations are solved again on the new mesh and the determination of the mesh repeated. Subsequent models are computed on the mesh based on the model at the previous time level; repeating the mesh determination and solution had little effect.

The distance r_1 from the centre of the innermost mesh point is calculated as

$$r_1 = 0.15\left(\sum_{i=1}^{5} \frac{1}{2\zeta_i}\left|\frac{d^2\zeta_i}{dr^2}\right|\right)^{-1/2}, \tag{C3}$$

evaluated at the centre. Here $\zeta_1 = p$, $\zeta_2 = T$, $\zeta_3 = X$, $\zeta_4 = m/r^3$ and $\zeta_5 = L/r^3$. This ensures that the ratio between the first and second term in the expansions of p, T, X, m and L is of order $(0.15)^2$.

The time step $\Delta t^{s+1} = t^{s+2} - t^{s+1}$ is determined from the change in the model from time level t^s to time level t^{s+1}. Specifically we use

$$\Delta t^{s+1} = \Delta y_{max}\left\{\max_n\left[(|y_i^{n,s+1} - y_i^{n,s}|)_{i=1,2,3,4},\right.\right.$$
$$\left.\left.\frac{|X^{n,s+1} - X^{n,s}|}{X^{n,s+1} + 0.05},\quad 200\,|X_3^{n,s+1} - X_3^{n,s}|\right]\right\}^{-1}; \tag{C4}$$

thus Δy_{max} is, roughly speaking, the maximum permitted change in the model between successive time levels. The time step following the initial model is taken to be very small, usually around 6×10^6 yr, in order to find the initial rate of change in the model, and the last two time steps are the same and are chosen to get a final model with the age of the present Sun.

Appendix D: The computation of oscillation periods

From the equations of linear adiabatic oscillations one may show that

$$\omega^2 \int_0^{r_s} \rho[\xi_r^2 + l(l+1)\xi_h^2] r^2\, dr$$
$$= \int_0^{r_s}\left[\Gamma_1 p D_1^2 + 2\frac{dp}{dr}\xi_r D_1 + \frac{1}{\rho}\frac{d\rho}{dr}\frac{dp}{dr}\xi_r^2\right] r^2\, dr + p'(r_s)\xi_r(r_s) r_s^2$$
$$+ \frac{4\pi G}{2l+1}\left\{-2\int_0^{r_s} r^{-(l-1)} D_2(r) \int_0^r r'^{l+2} D_2(r')\, dr'\, dr\right.$$
$$\left. + 2\rho(r_s)\xi_r(r_s) r_s^{-(l-1)} \int_0^{r_s} D_2(r) r^{l+2}\, dr - [\rho(r_s)\xi_r(r_s)]^2 r_s^3\right\}; \tag{D1}$$

here

$$\left.\begin{aligned} D_1 &= \frac{1}{r^2}\frac{d}{dr}(r^2\xi_r) - \frac{l(l+1)}{r}\xi_h, \\ D_2 &= \frac{1}{r^2}\frac{d}{dr}(r^2\rho\xi_r) - \frac{l(l+1)}{r}\rho\xi_h \end{aligned}\right\} \tag{D2}$$

are the amplitudes of $\mathrm{div}(\delta r)$ and $\mathrm{div}(\rho\delta r)$ respectively, and the notation is otherwise as in Christensen-Dalsgaard (1981). For radial oscillations equation (D1) may be considerably simplified, to give

$$\omega^2\int_0^{r_s}\xi_r^2\rho r^2\,dr = \int_0^{r_s}\left\{\Gamma_1 p r^4\left[\frac{d}{dr}\left(\frac{\xi_r}{r}\right)\right]^2 - r\xi_r^2\frac{d}{dr}[(3\Gamma_1-4)p]\right\}dr$$
$$+ r_s[3\Gamma_1 p(r_s)\xi_r(r_s) + r_s\delta p(r_s)]\,\xi_r(r_s). \tag{D3}$$

Equations (D1) and (D3) are well known in the case where the surface density of the equilibrium model is zero and the surface terms consequently vanish (*cf.* Ledoux & Walraven 1958).

It was shown by Chandrasekhar (1964) that if $\rho = 0$ on the surface equation (D1) is a variational expression for the squared frequency ω^2; in the radial case this result was obtained by Ledoux & Pekeris (1941). The variational property remains valid for general models, however, provided the oscillations satisfy the condition that the Lagrangian pressure perturbation vanish on the surface, i.e.

$$\delta p = 0 \qquad \text{at } r = r_s. \tag{D4}$$

Mathematically this follows from the symmetry of the operator defined by the equations of motion (Christensen-Dalsgaard 1981). From a physical point of view it reflects Hamilton's principle for the system consisting of the oscillating star; this system is conservative as the oscillations are adiabatic and isolated because of the condition (D4). Thus the change $\delta\omega$ in ω, evaluated from equations (D1) or (D3), corresponding to small changes $\delta\xi_r$ and $\delta\xi_h$ and ξ_r and ξ_h, is quadratic in $\delta\xi_r$ and $\delta\xi_h$.

As was first pointed out by Christensen-Dalsgaard *et al.* (1979) this suggests that a more accurate estimate of the frequency may be obtained by substituting computed eigenfunctions $\xi_r(r)$ and $\xi_h(r)$ into equations (D1) and (D2) for non-radial, or the computed $\xi_r(r)$ into equation (D3) for radial, oscillations. Let Π_V be the value of the period found from this estimate of ω, and Π_E the period found from the value of ω obtained as an eigenvalue of the system of oscillation equations. If a second-order scheme is used to integrate these equations we may then expect that the errors $\delta\Pi_V$ and $\delta\Pi_E$ in Π_V and Π_E satisfy

$$\delta\Pi_V \propto N^{-4}, \qquad \delta\Pi_E \propto N^{-2} \tag{D5}$$

where N is the number of mesh points. To attain the N^{-4} accuracy of Π_V the numerical differentiation in equations (D2) and (D3) and the numerical integration in equations (D1) and (D3) must be performed using schemes of sufficiently high order.

As was found numerically by Christensen-Dalsgaard *et al.* (1979) this procedure cannot be directly applied to high-order g modes. This may be understood by noting that the first integral on the right-hand side of equation (D1) can be rewritten as

$$\int_0^{r_s}\left[\frac{p}{\Gamma_1}\left(\frac{p'}{p}\right)^2 + \rho\mathcal{N}^2\xi_r^2\right]r^2\,dr, \tag{D6}$$

where

$$\mathcal{N}^2 = g\left(\frac{1}{\Gamma_1}\frac{d\ln p}{dr} - \frac{d\ln\rho}{dr}\right)$$

is the squared buoyancy frequency. For modes of low frequency p'/p is small compared with ξ_r/r (e.g. Cox 1980, p. 269), and so direct evaluation of the right-hand side of equation (D1), with D_1 found from ξ_r and ξ_h using equation (D2), leads to severe loss of accuracy due to cancellation. To avoid this problem we may instead calculate D_1 from the eigenfunction as

$$D_1 = -\frac{1}{\Gamma_1 p}\left(\rho\omega^2 r\xi_h + \frac{dp}{dr}\xi_r + \rho\Phi'\right); \tag{D7}$$

equation (D2) is then used to determine

$$\tilde{\xi}_h = \frac{1}{l(l+1)}\left[\frac{1}{r}\frac{d}{dr}(r^2\xi_r) - rD_1\right], \tag{D8}$$

which is substituted for ξ_h on the left-hand side of equation (D1). This procedure preserves the variational property while avoiding the problems encountered earlier, and was used for all calculations of g mode periods. Note, however, that for high-order p modes ξ_h is much smaller than either term on the right-hand side of equation (D8), and so the use of this equation is numerically ill-conditioned. Thus the two procedures are complementary.

To test these methods one may consider oscillations of polytropic models, whose structure can easily be calculated to any desired accuracy. We have verified that the dependence given in equation (D5) of the error on the number of mesh points is satisified for p and g modes in a polytropic of index 3 (*cf.* Christensen-Dalsgaard 1977). A particularly instructive case is the polytrope of index 0 whose eigenfrequencies are known analytically (Pekeris 1938). Fig. 4 shows relative errors in Π_V and Π_E of p modes of degree 0 and 2,

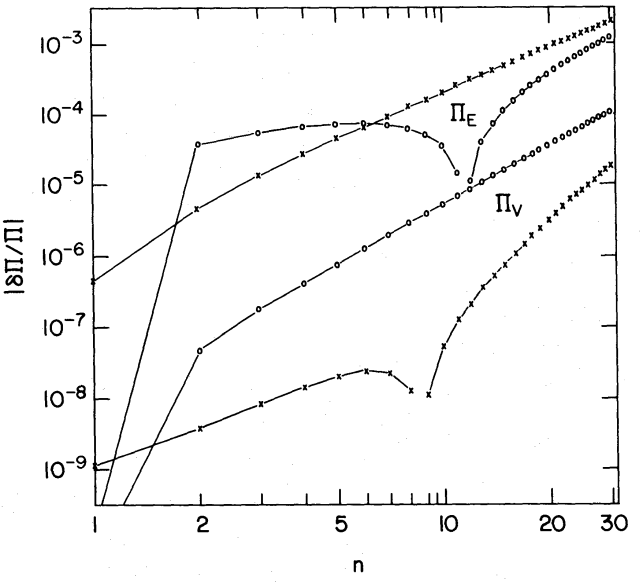

Figure 4. Relative errors in the periods of the modes $p_n(l = 0)$ (O–O–O) and $p_n(l = 2)$ (X–X–X) in the polytrope of index 0, as functions of n. Π_E is the period determined from the eigenfrequency and Π_V the period found from the variational expression. The oscillation calculation used 600 mesh points.

Table 5. Estimated relative errors $\delta\Pi_E/\Pi_E$ and $\delta\Pi_V/\Pi_V$ in the periods determined from the eigenfrequency and the variational expression, respectively, using 600 points in the oscillation calculation. The equilibrium model is model 1 of Table 1.

Mode	$\delta\Pi_E/\Pi_E$	$\delta\Pi_V/\Pi_V$
p_{29} ($l = 0$)	-2.98×10^{-3}	1.85×10^{-4}
p_{17} ($l = 0$)	-9.65×10^{-4}	6.55×10^{-5}
p_{28} ($l = 1$)	-2.85×10^{-3}	1.54×10^{-4}
p_{16} ($l = 1$)	-8.85×10^{-4}	6.42×10^{-5}
g_5 ($l = 1$)	-1.93×10^{-4}	-4.28×10^{-7}
g_{10} ($l = 2$)	3.04×10^{-4}	-1.46×10^{-6}
g_{14} ($l = 3$)	6.53×10^{-4}	-3.88×10^{-6}

computed for this model on a mesh with 600 points. It is evident that the error in Π_V is generally much smaller than the error in Π_E; for modes of order 30 (corresponding in a realistic solar model to the high-frequency end of the observed spectrum) Π_V is computed with a relative error of at most 10^{-4}. The differences between the errors for $l = 0$ and 2 probably arise because both the differential equations and the variational expression differ; the errors for modes with $l = 1$ and 3 are close to those for $l = 2$.

In a realistic model the variational property of ω^2 as computed from equations (D1) or (D3) no longer holds exactly, partly because of errors in the model and partly because the boundary condition (D4) is no longer used. In this case equation (D5) is replaced by

$$\delta\Pi_E \simeq \epsilon_E N^{-2}, \qquad \delta\Pi_V \simeq \epsilon_V^{(2)} N^{-2} + \epsilon_V^{(4)} N^{-4}; \tag{D9}$$

If the departures from the exact variational principle are small $\epsilon_V^{(2)}$ is much smaller than ϵ_E so that Π_V is still the more accurate. From computed values of Π_E for two different values of N, and computed values of Π_V for three different values of N, one may clearly estimate ϵ_E, $\epsilon_V^{(2)}$ and $\epsilon_V^{(4)}$. We have applied this to model 1 of Table 1, with $N = 600$, 300 and 200 and in this way obtained the estimates presented in Table 5 of the errors $\delta\Pi_E$ and $\delta\Pi_V$ in periods computed with $N = 600$. Although these estimates are somewhat uncertain, it is gratifying that they are, for given order n, of the same order of magnitude as the errors shown on Fig. 4. Thus the error in the computed Π_V, for given model, is probably less than 2×10^{-4} for modes in the 5 min range, and less than 5×10^{-6} for gravity modes of degree 1, 2 and 3 with periods close to 160 min.